

Supplementary Information

New vision of convection induced freckle formation theory in nickel-based superalloys by electron microscopy

New vision of convection induced freckle formation theory in nickel-based superalloys by electron microscopy

Shuai Wang^{1,#}, Yuliang Jia^{2,#}, Yongzhe Wang^{3,#}, Yongjia Zhang⁴, Lan Ma⁵, Feng Cheng¹, Yi Zeng³, Xu Shen⁴, Yingliu Du², Binghui Ge¹

¹Information Materials and Intelligent Sensing Laboratory of Anhui Province, Institutes of Physical Science and Information Technology, Anhui University, Hefei 230601, Anhui, China.

²Anhui Yingliu Hangyuan Power Technology Co., Ltd, Huoshan 237200, Anhui, China.

³The State Key Lab of High Performance Ceramics and Superfine Microstructure, Shanghai Institute of Ceramics, Chinese Academy of Sciences, Shanghai 200050, China.

⁴State Key Laboratory of Materials Processing and Die & Mould Technology, School of Materials Science and Engineering, Huazhong University of Science and Technology, Wuhan 430074, Hubei, China.

⁵Department of Nano-analysis, The Oxford Instruments Technology China, Shanghai 200233, China.

[#]Authors contributed equally.

Correspondence to: Prof. Binghui Ge, Information Materials and Intelligent Sensing Laboratory of Anhui Province, Institutes of Physical Science and Information Technology, Anhui University, Hefei 230601, Anhui, China. E-mail:

bhge@ahu.edu.cn; Prof. Yi Zeng, The State Key Lab of High Performance Ceramics and Superfine Microstructure, Shanghai Institute of Ceramics, Chinese Academy of Sciences, 1295 Dingxu Road, Shanghai 200050, China. E-mail:

zengyi@mail.sic.ac.cn

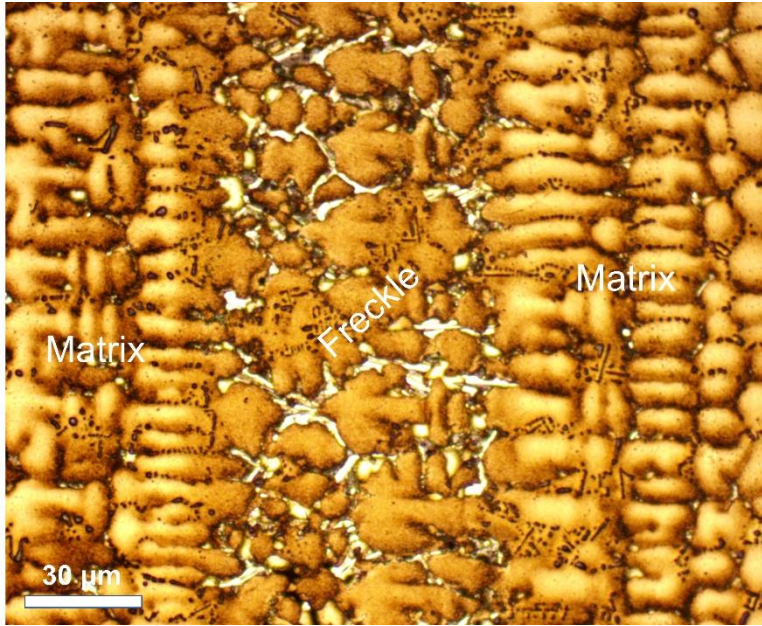


Figure S1. Metallographic structure image of freckle chain.

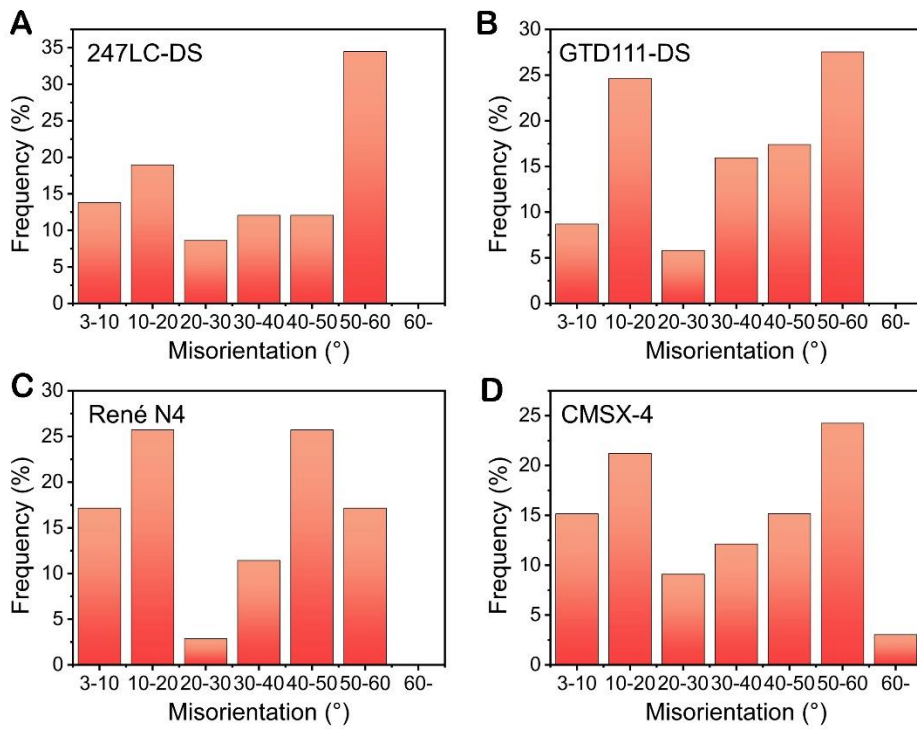


Figure S2. Individual statistical results of the misorientation of freckle grains relative to the matrix in four brands of alloys. (A-D) Statistical results of misorientation of freckle grains relative to the matrix in 247LC-DS, GTD111-DS, René N4 and CMSX-4, respectively.

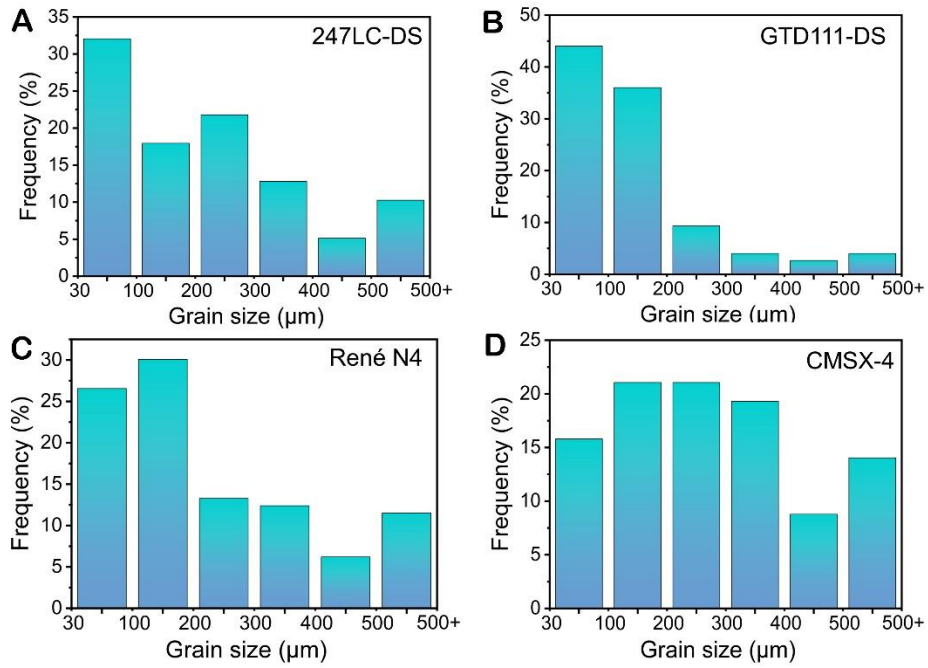


Figure S3. Individual statistical results of freckle grain size in four brands of alloys. (A-D) Statistical results of grain size in 247LC-DS, GTD111-DS, René N4 and CMSX-4, respectively.

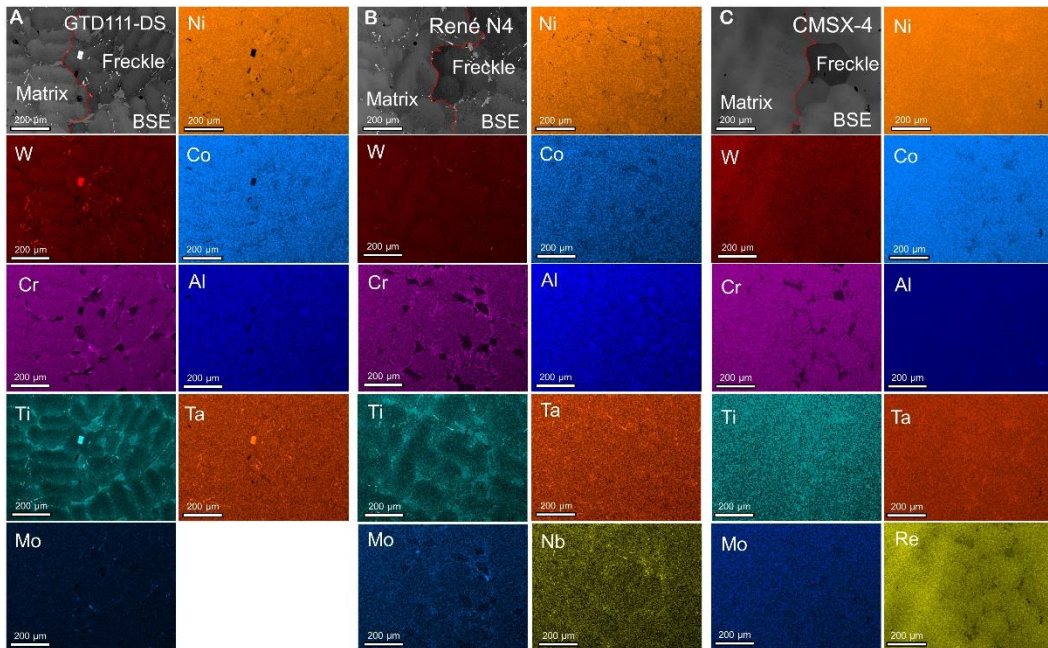


Figure S4. EDS maps of other three brands of alloys. (A-C) Statistical results of BSE image and EDS maps across the interface between the matrix and freckles in GTD111-DS, René N4 and CMSX-4, respectively.

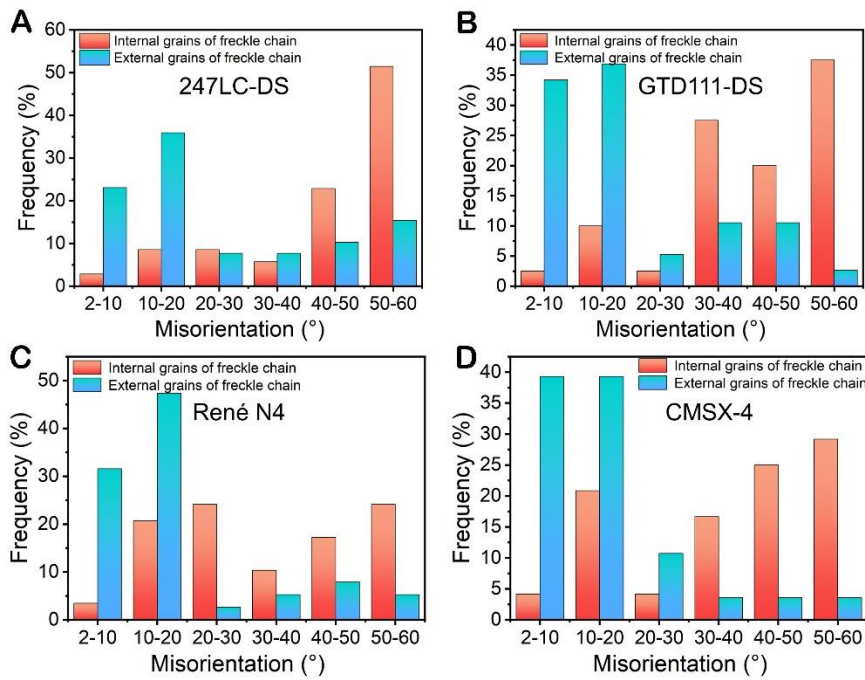


Figure S5. Individual statistical results of the MA distribution for the internal and external grains in four brands of alloys. (A-D) Statistical results of the MA distribution for the internal and external grains in 247LC-DS, GTD111-DS, René N4 and CMSX-4, respectively.

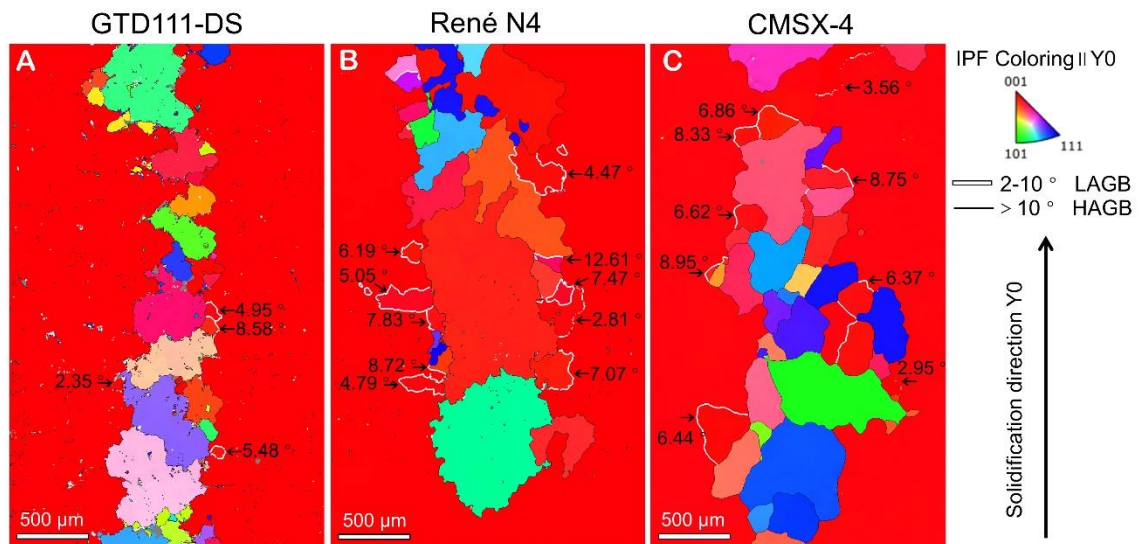


Figure S6. Orientation characterization of freckle grains of other three brands of alloys.

(A-C) Orientation maps of GTD111-DS, René N4 and CMSX-4, respectively, and LAGBs are highlighted with white lines and their MA are marked

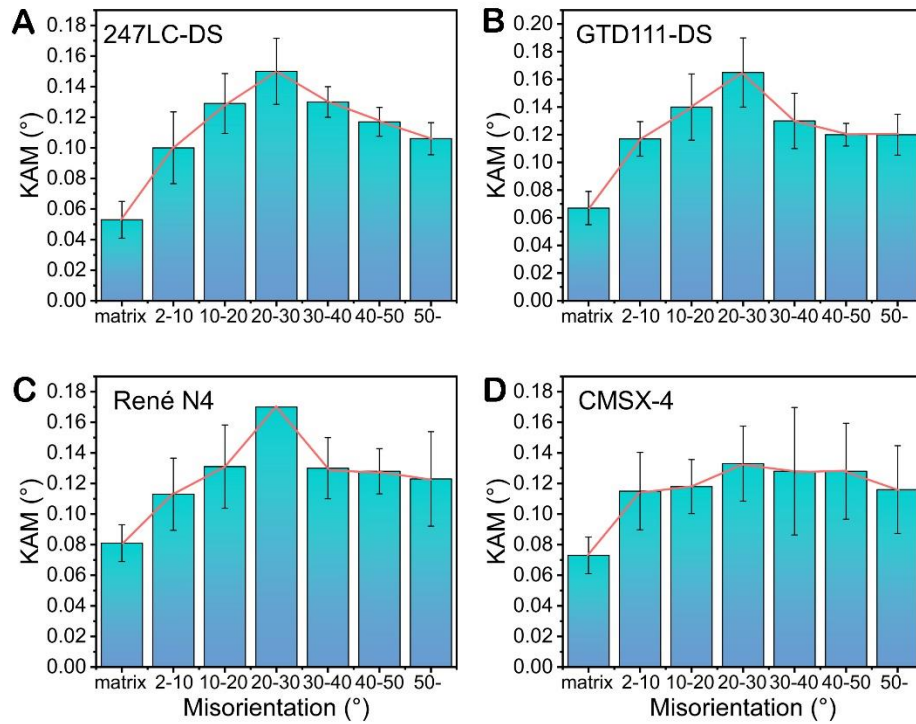


Figure S7. Individual statistical results of the KAM variation with MA in four brands of alloys. The orange curve is used to describe the trend. (A-D) Statistical results of the KAM variation with MA in 247LC-DS, GTD111-DS, René N4 and CMSX-4, respectively.

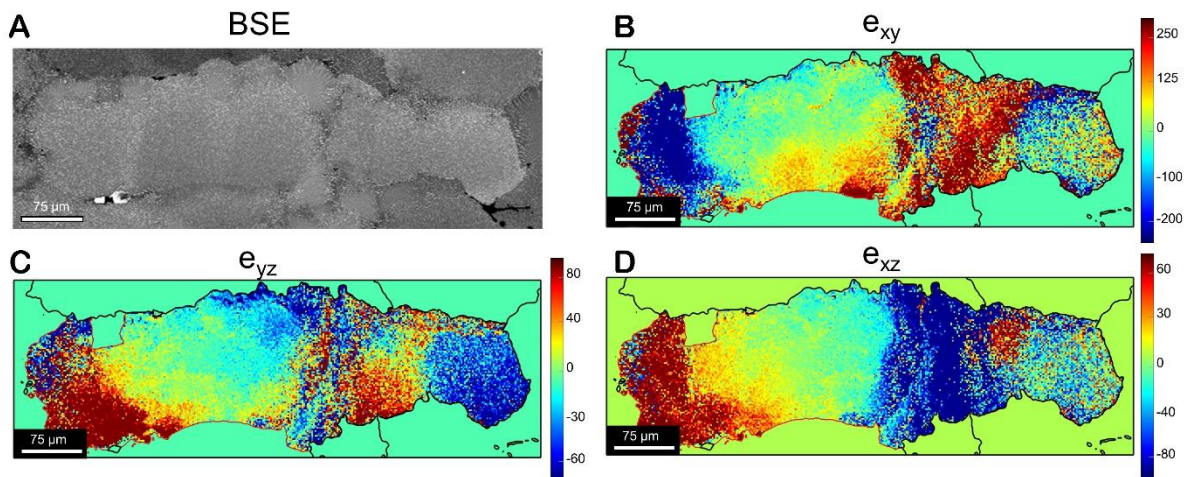


Figure S8. Shear stress distribution obtained by HR-EBSD. (A) BSE image of the freckle grain marked in red in Figure 3D. (B-D) Stress distribution of e_{xy} , e_{yz} , and e_{xz} , respectively.

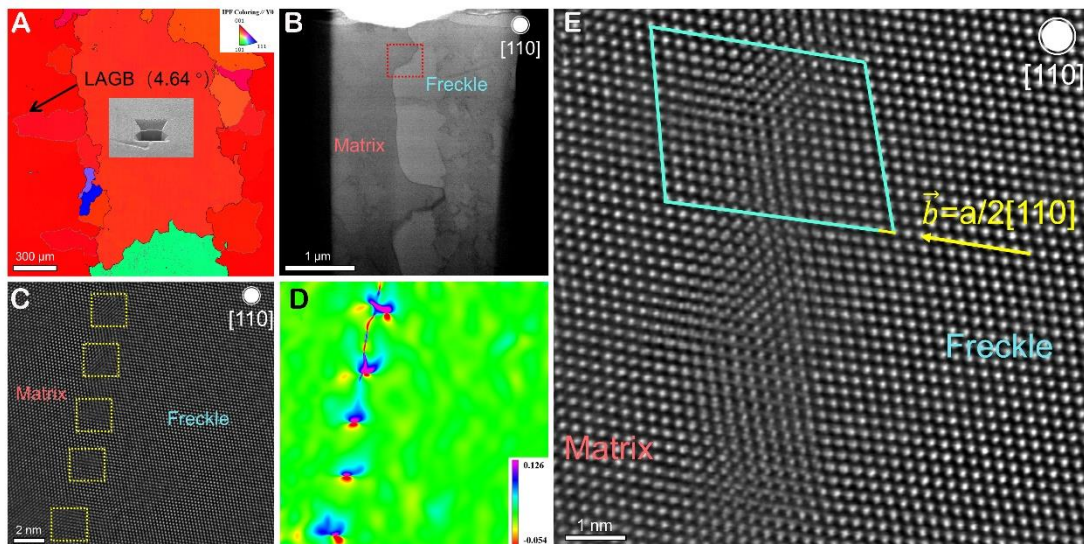


Figure S9. Characterization of LAGB in René N4 alloy along the orientation of [110]. (A) Orientation map obtained by EBSD and the sampling position of TEM marked with a black arrow, and the MA is 4.64°. (B) Low magnification BF-STEM image of LAGB. (C) High magnification HAADF images corresponding to the area marked by a red dashed line in (B), and continuous distortion regions marked with yellow dashed rectangles. (D) GPA image corresponding to (C) and the color bar is inset in the bottom right. (E) High magnification HAADF-STEM image of LAGB and Burgers vector determined by the Burgers circuit.

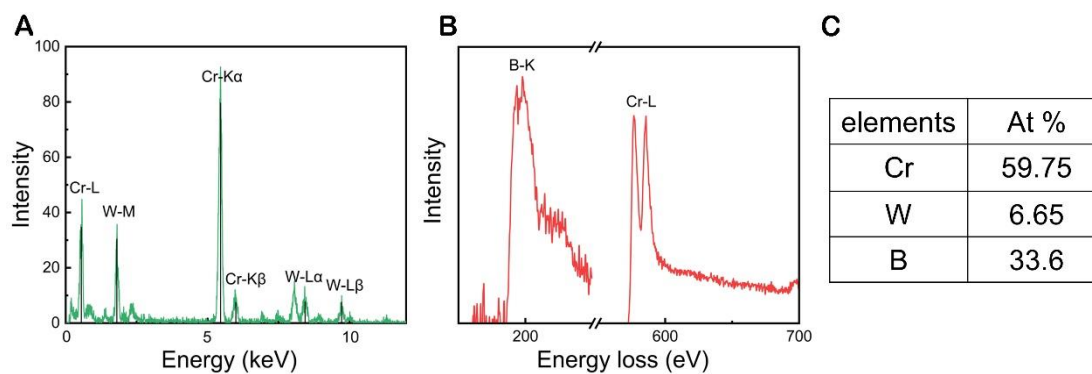


Figure S10. Composition determination of borides. (A-B) EDS and EELS spectra of boride 3. (C) Atomic percentage of borides.